Pion production from a critical QCD phase

N.G. Antoniou, Y.F. Contoyiannis, F.K. Diakonos,
A.I. Karanikas and C.N. Ktorides [a]

[a]Department of Physics, University of Athens, GR-15771 Athens, Greece

A theoretical scheme which relates multiparticle states generated in ultrarelativistic nuclear collisions to a QCD phase transition is considered in the framework of the universality class provided by the 3-D Ising model. Two different evolution scenarios for the QGP system are examined. The statistical mechanics of the critical state is accounted for in terms of (critical) cluster formation consistent with suitably cast effective action functionals, one for each considered type of expansion. Fractal properties associated with these clusters, characterizing the density fluctuations near the QCD critical point, are determined. Monte-Carlo simulations are employed to generate 'events', pertaining to the total system, which correspond to signals associated with unconventional sources of pion production.

1. Introduction

It is widely speculated that ultra-relativistic nucleus-nucleus (A+A) collisions offer an experimental methodology by which a transition from ordinary (confined) matter to a quark-gluon plasma (QGP) state can be transiently attained. In view of such a prospective it becomes imperative to identify specific experimental signals in the outcome of these collisions whose origin can be unmistakenly ascribed to a critical behaviour.

From a phenomenological point of view we can list three basic topics as the most relevant to such an investigation:

(a) How to pick up patterns in the multihadron (pion) states generated in A+A collisions from the central rapidity region and extract pertinent information from them.

(b) What is one's conception of the evolution picture taking place between the (presumed) formation of the quark-gluon plasma system and hadronization.

(c) In what way does the underlying microscopic theory, i.e., QCD, leave its imprint on the production patterns of hadrons.

There is a variety of attitudes that can be taken with respect to the above issues. Even though the present work focuses upon the last one, it is important to specify the adopted viewpoints on the other two as well.

In regard to (a), our premise draws its inspiration from the Bialas-Peschanski [1] approach to data analysis for large multiplicity events. The emphasis, here, lies on the possible presence of non-statistical deviations which can be uncovered from experimentally determined probability distributions. The idea is to look for big bursts from small regions (cells) of the phase space which signal unusual fluctuations of density, an occurence

that has been termed as search for intermittency. Such intermittent spiky events induce a dependence of the scaled moments of experimentally defined probability distribution $P(p_1, ..., p_n)$ on the size $\delta\Omega$ of each cell, according to some power-law. Searches for intermittency in multiparticle states resulting from A+A collisions have so far revealed only fluctuations due to Bose-Einstein interference. However, the question that still remains open is whether intermittency could be directly ascribed to a quark-hadron phase transition of second order. This is precisely the attitude that underlines our present approach, *i.e.* our intention is to propose a scheme according to which intermittency patterns in a multiparticle hadronic state are intimately linked with fluctuations which make their presence near the QCD critical point.

Concerning, next, the space-time evolution of the (plasma) system produced in the central rapidity region we shall adopt, for the most part, the picture promoted by Bjorken [2,3]. The basic idea is that, following the collision, a "central plateau" is formed comprised of a thin slab which contains quarks and gluons in (local) thermal equilibrium. The expansion is envisioned to be smooth enough so that conditions of thermal equilibrium persist on a locus which is monitored by a collection of inertial observers with relative velocities. A proper time (τ) dependence of all relevant thermodynamic quantities that describe the "fluid" emerges so that one writes $\varepsilon(\tau)$, $p(\tau)$, $\beta(\tau)$, respectively for energy and pressure densities and for inverse temperature. Dynamical evolution is thereby described by a sequence of a hyperboloidal, spacelike surfaces whose profile is specified by a hyperbolic section in the $t - z$ plane (z is the direction along which the collision takes place) and flat geometry in the transverse directions. This situation persists for a time scale of $\sim$ 10-20 fm/c $\left(\sim \beta_c A^{\frac{1}{3}}\right)$ at which point formation of primordial hadrons (mostly pions) occurs. As an alternative possibility to the above we shall consider, in Section 5, a spherically symmetric evolution of a centrally formed fireball of quarks and gluons. Our numerical studies will cover both scenarios.

The final issue, towards which the present paper basically addresses itself, concerns the interpolation between the underlying microscopic theory and observed patterns in the multihadron states generated by A+A collisions. In particular, we shall focus our efforts on determining possible imprints left by long range fluctuations, present in a critical quark-gluon system, on the produced multiparticle states. Evidence is, in fact, mounting from ongoing theoretical activity based on microscopic considerations which simulate QCD through specific models (*e.g.* that of Nambu and Jona-Lasinio), which lends overwhelming support to the existence of a critical point in the thermodynamical plane of temperature vs. chemical potential [4,7]. The latter is the remnant of a tricritical point occuring in the phase diagram of the ideal case $m_u = m_d = 0$ and from which a second order chiral phase transition curve originates belonging to the universality class of the O(4) σ-model [5]. For the realistic case where the up-down current quark masses are different from zero it marks the termination of a first order phase transition curve [6]. Such a point signals the onset of long range correlations and the relevant issue is to identify its universality class. It is widely believed that the latter is represented by the 3-D Ising model [7,8]. Under this assumption we shall adopt a strategy according to which the corresponding effective action $\Gamma[\sigma]$ is: a) accomodated on hyperboloidal surfaces of the type specified by Bjorken's picture for the space-time expansion of the plasma or b) adjusted to a spherical expansion scenario. Given that $\Gamma[\sigma]$ is a functional of a *classical* field, having resulted

from an integration over microscopic degrees of freedom, we shall propose that it plays the role of the free energy associated with sigma condensates.

From such a premise, the bulk of our effort will be to establish direct connections between the critical QGP system and observed patterns in hadron production. It is our aim to make specific predictions relating to the extensive experimental programme on heavy ions now in progress (SPS, RHIC, LHC), some of which have already been reported in previous, brief, expositions [9]. Our results will be summarized in an assortment of Monte-Carlo simulations stemming from the advocated theoretical approach. Given that intermittency effects in hadron production patterns are foremost in our minds, the significance of the presented output should be directly relevant to the goal of identifying clear experimental signals for the existence of a critical point in quark matter.

As can be surmised from the above remarks, our proposed scheme relies centrally on the idea that the observed patterns in hadron production have a component whose source is the large scale dynamics induced by the underlying microscopic theory at the critical point. At the same time, it constitutes an effort which stays close to an equilibrium frame of description[1], in juxtaposition with alternative approaches which place primary emphasis on the non-equlibrium aspects of the problem, see, *e.g.* [10].

Clearly, we cannot altogether avoid the out-of-equilibrium dynamical component entering the transition from the (critical) QGP to the hadronic state of the considered physical problem. In our scheme this matter enters in connection with the critical slowing down expected to occur between the critical, T_c, and freeze-out, T_f, temperatures - the latter marking the onset of the emergence of hadrons. Adopting a working assumption of the form $T_c \approx T_f$, owing to the fact that the specific heat diverges at the critical point, allows us to remain within the equilibrium frame of description. On the other hand, the (proper) time interval between the aformentioned two temperatures is *not* necessarily negligible. Clearly, dynamical matters related to critical slowing down effects present an interest of their own. We shall not, in this paper enter the discussion of issues related to dynamical scaling behavior.

Our paper is organized as follows. Section 2 is devoted to the presentation of the field theoretical framework within which we shall pursue the study of the critical system, assuming Bjorken's evolution picture for the QGP. In Section 3 we develop a Statistical Mechanical frame of description for the critical field system which relies on cluster formation. We proceed, in Section 4, to discuss the statistical content of the global system, setting the stage for the development of a Monte-Carlo generator for critical events that will be taken up in Section 6. In the interim, Section 5, we shall display the basic battery of formulas pertaining to the spherical evolution scenario for the QGP system. Section 6 addresses the quintessential issue regarding the generation of events with critical fluctuations as well as their identification in the profile of the produced pions which can be traced to a critical point of second order. In section 7 we present our numerical results by performing an event-by-event analysis in a large set of critical events and showing how our dedection algorithm of the critical fluctuations works in practice. Finally, section 8 contains concluding remarks.

[1]We shall not, in this paper, be preoccupied with precise dynamical accounts underlying the time development of the QGP system from its initial formation to its critical stage. Our basic concern is, simply, to justify our choices for the geometrical profile of the QGP state as the critical point is approached.

2. Adjustment of the 3-D Ising-model to Bjorken's evolution scenario

Our basic theoretical input is provided by the effective action of the 3-D Ising model $\Gamma[\sigma]$, which, following the analysis of [11], adequately represents QCD in the vicinity of the second order critical point $T = T_c, \mu = \mu_c$ (as the endpoint of a first-order phase transition line) resulting by taking into account the finite mass for up and down quarks. Thus, provided driving parameters of the model (e.g., temperature, coupling constant, etc.) are on or near their critical values, $\Gamma_c[\sigma]$ can be looked upon as the free energy for the critical system.

According to our viewpoint the aformentioned free energy incorporates the sigma field condensates, $\sigma \sim \langle \overline{q}q \rangle$, in thermal equilibrium near the critical temperature $T \approx T_c$. As already mentioned in the introductory section, for the most part of this work we shall feel phenomenologically justified to keep our considerations on a strictly equilibrium level by taking into account that the freeze-out temperature T_f, at which one meets the asymptotic states of the produced hadronic system, is very close to the critical temperature ($T_c \approx T_f$). This means that we shall view the second order phase as a direct interpolation between the condensates and the asymptotic hadronic states.

Under conditions of strict local equilibrium the thermodynamics of the condensates is described, in the ordered phase ($T \leq T_c$), by the free energy which we express, at $T = T_c$, as follows

$$\Gamma_c[\sigma] = T_c^{-1} \int d^3\vec{x}[\frac{1}{2}(\nabla\sigma)^2 + gT_c^4(T_c^{-1}\sigma)^{\delta+1}] \tag{1}$$

where δ is the isothermal critical exponent and g is a dimensionless coupling. The field σ has a dimension $\sigma \sim (\text{length})^{-1}$. The parameters (g, δ) are universal and specify the critical equation of state: $\frac{\delta\Gamma_c}{\delta\sigma} \sim g\sigma^\delta$. For the Ising 3-D universality class we have $\delta \approx 5$, due to the smallness of the anomalous dimension [13], and $g \approx 1.5 - 2.5$ as obtained in [12,13].

Our next concern is to cast the effective action $\Gamma_c[\sigma]$ in a manner that is explicitly adapted to Bjorken's inside-outside cascade picture for the plasma expansion. For this purpose we introduce rapidity and proper time coordinates (ξ, τ) so that the longitudinal space element, corresponding to a local observer in a comoving system, becomes $dx_{||} = \tau d\xi$. With this choice and for the purpose of describing the clusters formed at $T = T_c$, the "longitudinal" integration occurs along the critical hyperbola $\tau = \tau_c$. We thereby obtain the following expression for the effective action which furnishes an appropriate account for the system as the critical temperature is reached:

$$\Gamma_c[\sigma] = \frac{1}{C_A} \int_\Delta d\xi \cosh\xi \int_{S_\perp} d^2\mathbf{x}_\perp \left[\frac{1}{2\cosh\xi} \left(\frac{\partial\sigma}{\partial\xi} \right)^2 + \frac{\tau_c^2}{2} (\nabla_\perp\sigma)^2 + gT_c^4 C_A^2 (T_c^{-1}\sigma)^{\delta+1} \right] \tag{2}$$

where Δ is the rapidity size, $S_\perp$ is the transverse area of the system and $C_A = \frac{\tau_c}{\beta_c}$.

One notices that, through (2), the system has been accomodated on a space-like hyperboloidal surface which is flat in the transverse directions x, y and intersects the $t-z$ plane as a hyperbola (z is the collision direction). The monitoring of the field system in our case calls for a collection of local inertial observers who must put their data together in order to construct its full description. This occurence is ideally suited to the Bialas-Peschanski

scenario concerning the detection of intermittency patterns in the multiparticle hadronic production. Within this picture it turns out that the total rapidity size Δ in eq.(2) should be replaced by a narrow strip $\Delta\xi$ in rapidity around a local observer. Furthermore, we are free to choose $\Delta\xi \leq 1$ and make use of the approximation $\cosh\xi \approx 1$ which is valid within 10 %.

As already stated our central goal is, assuming that $T_c \approx T_f$, to formulate correspondences between field quantities associated with the critical system, on the one hand and hadronic observables on the other. On the field theory side the relevant issue concerns the statistical account of the macroscopic system comprised of condensates. One needs to define a statistical weight factor appropriate for the equilibrium situation in hand. A convenient way in terms of which one might proceed to accomplish this task is to employ a coherent state analysis (see, e.g., [14]) which, by definition, pertains to collective fields. Let us recall that coherent states are eigenstates of field operators, being a superposition of Fock states of arbitrary particle content. One writes (the *tilde* on top signifies an operator)

$$\tilde{\sigma}(x)|\sigma> = \sigma(x)|\sigma>, \tag{3}$$

where the $|\sigma>$ denote coherent (classical, in effect) states of the field σ. Our basic assumption is that the density matrix associated with the partition function is diagonal in the coherent-state representation.

In turn, the average multiplicity $< n >$ of sigmas is given by

$$< n >= \int \mathcal{D}[\sigma] \left[\int_V d^2\vec{x}_\perp d\xi \sigma^2(\vec{x}_\perp, \xi)\right] e^{-\Gamma_c[\sigma]} / \int \mathcal{D}[\sigma] e^{-\Gamma_c[\sigma]} \tag{4}$$

The above formulas will be centrally relied upon in our subsequent analysis. They, in fact, serve as a bridge between an original microscopic description - which has been given a macroscopic, collective content by integrating out a huge number of degrees of freedom - and the statistical treatmeant of fluctuations in the resulting critical, collective system [14].

3. Statistical Mechanics of the critical system: cluster formation

To the extent that we shall be restricting ourselves to a strictly equilibrium mode of description, the strategy by which we propose to study the critical system is through cluster formation. The physical picture we attach to (critical) clusters is that they represent distributions of primordial hadrons (massless sigmas) whose growth is driven by the transition from the QGP to the hadronic state of matter. From a formal, mathematical, viewpoint such clusters serve as entities which interpolate between critical exponents characterizing the plasma system on the one hand and fractal dimensions associated with the hadronic (pion) emission patterns on the other.

The 3-D configurations representing the clusters will be assembled as follows. First, their one-dimensional (longitudinal) profile along the rapidity axis will be considered, given that this is where the bulk of the dynamical effects is encountered. Next, we shall proceed to investigate their transverse fractal properties by freezing the rapidity variable. The cartesian synthesis of a given cluster, provides a well defined picture of a cluster's

constitution. The latter, certainly adheres to the cylindrical (with respect to the rapidity axis) and Lorentz (save at the edges) symmetries which characterize the overall system.

The projection onto the rapidity direction is furnished by the 1-D effective action functional:

$$\Gamma_c^{(1)}[\hat{\sigma}] = \frac{\pi R_\perp^2}{\beta_c \tau} \int_{\Delta\xi} d\xi \left[\frac{1}{2} \left(\frac{\partial \hat{\sigma}}{\partial \xi} \right)^2 + g C_A^2 \left(\hat{\sigma}^2 \right)^{\frac{\delta+1}{2}} \right] \tag{5}$$

where $\Delta\xi$ is the rapidity strip around the local observer at $\xi = 0$ and $R_\perp$ the transverse radius of the system at $T = T_c$, while $\hat{\sigma}$ denotes a dimensionless σ-field ($\hat{\sigma} = T_c^{-1}\sigma$).

For notational ease we make the identifications

$$g_1^{(1)} = \frac{\pi R_\perp^2}{\beta_c \tau_c} \quad ; \quad g_2^{(1)} = g C_A^2 \tag{6}$$

which recast Eq.(5) into the following generic form

$$\Gamma_c^{(1)}[\hat{\sigma}] = g_1^{(1)} \int_{\Delta\xi} d\xi \left[\frac{1}{2} \left(\frac{\partial \hat{\sigma}}{\partial \xi} \right)^2 + g_2^{(1)} \left(\hat{\sigma}^2 \right)^{\frac{\delta+1}{2}} \right] \tag{7}$$

The local system is considered as *open*, i.e. it communicates with the total system, so that no boundary conditions are imposed on it. In turn, this implies that we are free to consider analytic continuation of (7), with respect to $\Delta\xi$, which will furnish scaling properties of extensive thermodynamical quantities registered by the local (sub)system as its size is being varied. We emphasize that our specification $\xi = 0$ has been made strictly for notational ease; any local oberver, located at $\xi = \xi_i$ is equally acceptable, due to Lorentz invariance, provided that the said observer is not too close to the boundaries of the total system.

For heavy nuclei, $\frac{\pi R_\perp^2}{\beta_c \tau_c} \gg 1$, the evaluation of the partition function of the subsystem

$$Z_c = \int \mathcal{D}[\hat{\sigma}] e^{-\Gamma_c[\hat{\sigma}]} \tag{8}$$

is dominated by saddle point configurations. In what follows we drop, for simplicity of notation, the hat used to indicate dimensionless quantities.

There emerge instanton-like solutions of the classical equations of motion [17]

$$\ddot{\sigma} - (\delta + 1) g_2^{(1)} \sigma^\delta = 0 \tag{9}$$

which are classified according to total energy

$$E = \frac{1}{2}\dot{\sigma}^2 - g_2^{(1)} |\sigma|^{\delta+1} \tag{10}$$

and size ξ_0.

Now, for a given solution it follows, in a straight forward manner, that a suppression term $e^{-E\Delta\xi}$ factorizes in the expression for the partition function, hence the dominant contributions correspond to configurations with vanishing energy. Under these circumstances one obtains the following analytic expression for the instanton-like solution

$$\sigma(\xi) = \left[\frac{\sqrt{2}}{(\delta - 1)\sqrt{g_2^{(1)}}} \right]^{\frac{2}{\delta-1}} |\xi - \xi_0|^{-\frac{2}{\delta-1}} \tag{11}$$

As a function of the varying size $\Delta\xi$ the effective action takes the form

$$\Gamma_c(\Delta\xi;\xi_0) \;=\; \frac{2g\pi R_\perp^2}{\beta_c\tau_c}C_A^2\int_{\Delta\xi}[\sigma(|\xi-\xi_0|]^{\delta+1}d\xi \tag{12}$$

In order to suppress large contributions to the free energy, hence practically zero contributions to the partition function, we impose the restriction that the "instanton" size be much larger than the size of the local system, i.e. $\Delta\xi \ll \xi_0$. As a result, we obtain approximately constant solutions in the domain $\Delta\xi$, of the form

$$\sigma \approx \left[\frac{\sqrt{2}}{\xi_0\sqrt{g_2^{(1)}(\delta-1)}}\right]^{\frac{2}{\delta-1}} \tag{13}$$

The computation of the partition function is now reduced to an integration over the "instanton" size. We let physical insight guide the relevant calculation by thinking as follows. Consider an extensive variable M associated with the field configuration of the critical system in the region monitored by our local observer, including its analytic continuation. Specifically, we choose the quantity $M=\int_0^{\Delta\xi}[\sigma(x)]^2dx$ which furnishes, according to eq.(4), the multiplicity $< n(\Delta\xi) >=< \int_0^{\Delta\xi}[\sigma(x)]^2dx >$ of sigmas within the domain of extent $\Delta\xi$. Moreover, we introduce the concept of a *cluster* of radius $\Delta\xi$ as an object with geometrical properties built up through the statistical average over configurations corresponding to values of M greater than a minimum value μ (for the case at hand $\mu=1$). Referring to (4) and (12) this average is determined as follows

$$\begin{aligned} < \int_0^{\Delta\xi}[\sigma(x)]^2dx > \;\; &= \;\; \frac{A^2\frac{\delta-1}{\delta-3}}{Z}\int_{\Delta\xi}^{(A^2\Delta\xi/\mu)^{\frac{\delta-1}{4}}} d\xi_0\,\xi_0^{-\frac{\delta+1}{\delta-1}}\left[\xi_0^{\frac{\delta-3}{\delta-1}}-(\xi_0-\Delta\xi)^{\frac{\delta-3}{\delta-1}}\right] \\ &\quad\times\exp\left\{-G_1\frac{\delta-1}{\delta+3}\left[(\xi_0-\Delta\xi)^{-\frac{\delta+3}{\delta-1}}-\xi_0^{-\frac{\delta+3}{\delta-1}}\right]\right\} \end{aligned} \tag{14}$$

where $G_1\equiv 2g_1^{(1)}g_2^{(1)}A^{\delta+1}$ and $A=[g_2^{(1)}/2(\delta-1)^2]^{-\frac{1}{\delta-1}}$.

It can now be explicitly shown [17] that, for $G_1\gg 1$, three characteristic regions can be clearly identified with respect to the behaviour of the integral on the right hand side of (14):

$$\begin{aligned} \Delta\xi \ll \Delta_d \qquad &; \qquad < n(\Delta\xi) > \sim const. \\ \Delta_d \ll \Delta\xi \ll \Delta_u \qquad &; \qquad < n(\Delta\xi) > \sim (\Delta\xi)^{\frac{\delta-1}{\delta+1}} \\ \Delta\xi \gg \Delta_u \qquad &; \qquad < n(\Delta\xi) > \sim (\Delta\xi)^{\frac{\delta-5}{\delta-1}} \end{aligned} \tag{15}$$

where

$$\Delta_d \equiv A^{-2\frac{\delta+1}{\delta-1}}G_1^{\frac{2}{\delta-1}}\mu^{\frac{\delta+1}{\delta-1}} \quad ; \quad \Delta_u \equiv G_1^{\frac{\delta-1}{\delta+3}} \tag{16}$$

serve as the lower (Δ_d) and the upper radius (Δ_u) of a cluster centered around $\xi=0$.

There follows a fractal structure for the critical clusters with mass dimension

$$d_F^{(1)} = \frac{\delta-1}{\delta+1} \tag{17}$$

Turning our attention to the two-dimensional, transverse profile of the critical system we encounter the effective action functional

$$\Gamma_c^{(2)}[\sigma] = C_A \Delta \int_\perp d^2x_\perp \left[\frac{1}{2} (\nabla_\perp \sigma_\perp)^2 + g \left(\sigma^2 \right)^{\frac{\delta+1}{2}} \right] \tag{18}$$

where $\perp$, as subscript to the integral, serves to denote transverse size and Δ furnishes the total rapidity.

The form of the above expression is a two-dimensional analogue of (7) with corresponding parameters

$$g_1^{(2)} = C_A \Delta \quad ; \quad g_2^{(2)} = g \tag{19}$$

The counterpart of eq.(15) now reads

$$\begin{aligned} R \ll R_d \quad &; \quad < n_\perp(R) > \sim const. \\ R_d \ll R \ll R_u \quad &; \quad < n_\perp(R) > \sim R^{2\frac{\delta-1}{\delta+1}} \\ R \gg R_u \quad &; \quad < n_\perp(R) > \sim R^{2-\frac{4}{\delta-1}} \end{aligned} \tag{20}$$

where

$$R_d = G_2^{\frac{1}{2\delta}} A_2^{\frac{\delta+1}{2\delta}} \quad ; \quad R_u = \beta_c G_2^{\frac{\delta-1}{4}} \tag{21}$$

with $G_2 = 2\pi g_1^{(2)} g_2^{(2)} A_2^{\delta+1} \left(\frac{\delta+3}{4} \right)$ and $A_2 = ((g_2^{(2)}/4)(\delta-1)^2(\delta+1))^{-\frac{1}{\delta-1}}$. In analogy with eqs.(15) we conclude from eqs.(20) the formation of fractal clusters in transverse space with mass dimension $d_F^{(2)} = \frac{2(\delta-1)}{\delta+1}$ in the range $R_d \ll R \ll R_u$. The 3-D cluster is constructed following our original considerations according to which this object is roughly confined within a cylinder with radius R_u in transverse space and size $2\Delta_u$ in rapidity. This realization has the cartesian product form (rapidity $\otimes$ transverse space) and it is consistent with longitudinal expansion of the original system.

Referring to eq.(4), with $\Gamma_c[\sigma]$ given by (5), we estimate the average multiplicity for the 3-dimensional cluster to be [15]:

$$< n >_{cl} = \frac{\Gamma(\frac{3}{\delta+1})}{\Gamma(\frac{1}{\delta+1})} \left(\frac{V}{V_o} \right)^{\frac{\delta-1}{\delta+1}} \tag{22}$$

with $V = 2\pi R_u^2 \Delta_u$ and $V_o = \beta_c^2 \sqrt{2gC_A}$.

4. Multi-cluster description of the global system

Assuming that the entire critical system is a cylinder with rapidity size Δ and transverse radius $R_\perp$ we can calculate the mean number of 'cylindrical' clusters with rapidity size $2\Delta_u$ and transverse radius R_u contained in the global system. Denoting this number by N we determine $N = N_\parallel \times N_\perp$, where $N_\parallel$ denotes the number of clusters in rapidity and $N_\perp$ in transverse space, respectively. Using the fact that $\kappa = \frac{\delta+1}{2} \approx 3$ for the Ising 3-D universality class [12,13] we estimate, from the previous analysis, these numbers as:

$$\begin{aligned} N_\parallel &= \frac{\Delta}{2\Delta_u} = \frac{2\Delta\tau}{\sqrt{\pi} R_\perp} \left(\frac{g}{2} \right)^{1/4}, \\ N_\perp &= \left(\frac{R_\perp}{R_u} \right)^2 = \left(\frac{12\sqrt{6g} R_\perp}{\pi \Delta\tau} \right)^2 \end{aligned} \tag{23}$$

It follows that the 3-D critical system appears as an almost cylindrically symmetric[2] arrangement of, in the mean, N clusters. Each cluster (of size $2\Delta_u$ in rapidity and R_u transverse radius) has a fractal mass dimension d_F decomposed as the cartesian product $d_F = d_F^{(1)} + d_F^{(2)}$ of two fractals in the corresponding subspaces. We also observe that the size of the clusters in rapidity is relatively small, $\Delta_u = \frac{\sqrt{\pi}}{4}\left(\frac{R_\perp}{\tau}\right)$, justifying a posteriori the approximation $\cosh\xi \approx 1$ made in eq.(2).

The complete analysis calls for the power law underlying the behavior of the density-density correlation function $\rho(\xi,0) =< \rho(\xi)\rho(0) >$ in the scaling region. Differentiating the mean multiplicity, given by eq.(22), with respect to rapidity we are led [15] to

$$\rho(\xi,0) = (\frac{4}{27\pi g C_A})^{1/3}\beta_c^{-2}\frac{\Gamma(1/2)}{\Gamma(1/6)}|\xi|^{-1/3}|\frac{\vec{x}_\perp}{\beta_c}|^{-2/3} \tag{24}$$

As already mentioned, the fractal dimension emerging from the power-laws in rapidity space is given by $d_F^{(1)} = \frac{\kappa-1}{\kappa}$ and is valid in the scaling region $\delta_o(\equiv \Delta_d) \ll |\xi| \leq \Delta_u$.

In the presence of $N_\parallel$ non-overlapping sources, located along the rapidity direction at random points $\xi_1, ..., \xi_{N_\parallel}$, the corresponding partition function reads:

$$Z_{N_\parallel} = \sum_{\xi_1,...,\xi_{N_\parallel}} \prod_{i=1}^{N_\parallel - 1}\left[-\delta_o^{\kappa-1}\left(\frac{\pi R_\perp^2}{\beta_c^2}\right)^\kappa \int_{\Delta\xi_i} d\xi (< \sigma^2 >)^\kappa\right], \tag{25}$$

which leads [16] to the following distribution for the given multiplicity $N_\parallel$:

$$P(\xi_1, ..., \xi_{N_\parallel}) = \left(\frac{\Delta + 2\xi_1}{\delta_o}\right)^{-\frac{1}{2\gamma}}\left(\frac{\Delta - 2\xi_{N_\parallel}}{\delta_o}\right)^{-\frac{1}{2\gamma}}\prod_{i=2}^{N_\parallel}\left(\frac{\xi_i - \xi_{i-1}}{\delta_o}\right)^{-\frac{1}{\gamma}} \tag{26}$$

where $\gamma \equiv \left[\frac{9}{2}\Gamma\left(\frac{2}{3}\right)\right]^3$, with the assumed ordering being $-\frac{\Delta}{2} \leq \xi_1 \leq ... \leq \xi_{N_\parallel} \leq \frac{\Delta}{2}$. One readily notes that the largeness of γ allows us to regard the chain of clusters along the rapidity direction as a collection of practically non-interacting objects. This occurence will greatly facilitate, later on, our numerical simulations.

Unlike the rapidity case, fluctuations associated with transverse space are not directly observable in heavy ion experiments. What actually *is* observed is the pion distribution in the transverse momentum space. The need, therefore, arises to transform the geometrical picture valid for the transverse space to the corresponding picture in transverse momentum space. The two spaces are connected at the level of the density-density correlation through a Fourier transform:

$$\tilde{\rho}(\vec{p}_T) \sim \int d^2x_\perp e^{i\vec{p}_T\cdot\vec{x}_\perp}\ \rho(\vec{x}_\perp, 0) \tag{27}$$

where $\rho(\vec{x}_\perp, 0)$ is the density-density correlation for the sigmas in the transverse space projection of a critical cluster with center at $\vec{x}'_\perp = 0$ and $\tilde{\rho}(\vec{p}_T)$ the corresponding density-density correlation in the transverse momentum space. The latter is, by definition, related to the gradient of the mean multiplicity $< n_\perp(R) >$, see eqs.(20), with respect to R.

[2]We say 'almost' because the individual clusters are not supposed to behave as rigid structures; they can deform, due to the presence of neighbouring clusters, both in transverse and in rapidity directions.

Setting $R = |\vec{x}_\perp|$ we obtain

$$\rho(\vec{R}, 0) \sim \frac{1}{R}\frac{\partial < n(R) >}{\partial R} \sim R^{-\frac{2}{\kappa}} \tag{28}$$

Performing the Fourier integration, according to (27), we arrive at the following power-law for the density-density correlation in the transverse momentum space:

$$\tilde{\rho}(\vec{p}_T) \sim |\vec{p}_T|^{\frac{2(\kappa-1)}{\kappa}} \tag{29}$$

In analogy to the space description of the 3-D system, we now consider a collection of cylindrical clusters in the transverse momentum $\otimes$ rapidity space. The number of clusters in the transverse momentum projection is $N_\perp$ given by eqs.(23). Finally, the multiplicity of hadrons within one cluster is given by eq.(22).

In order to complete the description of the critical system in the transverse momentum we need an additional phenomenological input. We adopt the following assumptions:

- The centers of the clusters in the transverse momentum space $p_{T,i}$ are random variables distributed according to an exponential law:

$$f(p_T) = \frac{2}{\pi < p_T >^2} e^{-\frac{2p_T}{< p_T >}} \tag{30}$$

- The net transverse momentum flow through the clusters is suppressed:

$$\sum_{i=1}^{N_\perp} \vec{p}_{T,i} = 0 \tag{31}$$

where $< p_T >$ is the mean transverse momentum which can be approximated to: $< p_T > \approx 2T_c = 280\ MeV$. The size $|\Delta\vec{p}_\perp|$ of each cluster in the transverse momentum space is determined by the minimum length scale R_d in the transverse configuration space and is given by the relation [15]:

$$|\Delta\vec{p}_\perp| = \frac{T_c}{2}(\frac{R_\perp}{\tau})^{1/2}(\frac{g}{2})^{-3/8}(\frac{\pi^3}{C_A})^{1/4} \tag{32}$$

Having exhibited the portrait of the critical system according to the longitudinal evolution scheme, we can now turn our attention to the spherical mode of expansion. This we shall do in the following section through a display of a minimum of formalism.

5. Spherical evolution

In the present section we shall consider a different evolution scenario according to which the geometry of the $A+A$ collision is spherical. More specifically, we consider the situation where, following the collision, a fireball of spherical size is formed which expands radially outwards. As a result, the sigmas are now distributed inside a spherical cluster.

The starting point of our analysis is, once again, the 3-D effective action (1). Following a similar procedure with the one applied for the cylindrical geometry we find that the average multiplicity $< N_\sigma >$ is given by

$$< N_\sigma >= Z^{-1} \int \mathcal{D}[\sigma] e^{-\Gamma_c[\sigma]} (\beta_c^{-1} \int d^3 r \sigma^2(r)) \tag{33}$$

where the insertion of the factor β_c^{-1} has been made on dimensional grounds since $dim[\sigma^2] = (length)^{-2}$ and $< N_\sigma >$ must be dimensionless.

The partition function at $T = T_c$, with the scalar particles (σ) in a spherical volume $V(\leq (4/3)\pi R_u^3)$, now has the form

$$Z(N_\sigma, V, T_c) = N_\sigma^{-1/2} \exp(-(\frac{V}{V_o})^{\kappa-1} N_\sigma^\kappa) \tag{34}$$

where $V_o = (2g)^{\frac{1}{\kappa-1}} \beta_c^3$.

The upper limit R_u of the cluster can be computed directly from [17]. For the $D = 3$ case the anomalous dimension η of the sigma-field is involved in the resulting expression. We obtain $R_u = G_3^{-\frac{1}{q}}$ with $q = 3 - \frac{(2+3\eta)\kappa}{2}$ and $G_3 = \sqrt{\frac{2}{g_2^{(3)}}} \frac{\pi}{3} g_1^{(3)}$ [17]. For small η ($\eta \ll 1$) we find that $R_u \to \infty$. Accordingly, we can consider the whole system as being comprised of only one cluster with radius R_u. The average multiplicity $< N_\sigma >$ in this cluster, as a function of the volume V, follows from (34) and is given by

$$< N_\sigma >= \frac{\Gamma(\frac{3}{2\kappa})}{\Gamma(\frac{1}{2\kappa})} \left(\frac{V}{V_o}\right)^{\frac{\kappa-1}{\kappa}} \tag{35}$$

The above equation implies that there is a minimal volume scale, $V = V_o$, where self-similarity breaks down.

On general grounds, the fractal dimension in R^3-space is given by $d_F = 3\frac{\kappa-1}{\kappa}$ if we neglect η. Taking η into account (≈ 0.034 [13]) we obtain $d_F = 1.98$. Thus if we were to project this fractal onto rapidity and transverse space, respectively, we would not find corresponding fractal configurations since the dimensions of the spaces upon which we project are smaller or nearly equal to d_F [18].

To complete our considerations in configuration space we give the expression for the density-density correlation function which obeys the following characteristic power-law

$$< \rho(r)\rho(0) >= \frac{\Gamma(\frac{3}{2\kappa})}{\Gamma(\frac{1}{2\kappa})} (\frac{8\pi g}{3})^{-\frac{1}{\kappa}} \beta_c^{\frac{3-2\kappa}{\kappa}} r^{-\frac{3}{\kappa}} \tag{36}$$

Turning our attention to momentum space, the pattern is again a spherical cluster with center at $\vec{p} = 0$. The corresponding radius is determined by the lower limit R_d of the cluster size in configuration space, *i.e.* $|\Delta\vec{p}| \sim R_d^{-1}$. On the other hand, R_d is determined by the minimal volume $V_o = (4/3)\pi R_d^3$. It follows that:

$$|\Delta\vec{p}| \approx \left(\frac{2^{\frac{2\kappa-3}{\kappa-1}}\pi}{3g^{\frac{1}{\kappa-1}}}\right)^{1/3} \beta_c^{-1} \tag{37}$$

and for $g \approx 2$, we estimate $|\Delta\vec{p}| \approx 150\ MeV$. The fractal dimension in momentum space is $\tilde{d}_F = 3 - d_F = 3(1 - \frac{\kappa-1}{\kappa})$ and, the momentum distribution of sigmas inside the cluster is determined through the density-density correlation:

$$< \tilde{\rho}(|\vec{p}|)\tilde{\rho}(0) > \sim |\vec{p}|^{-3\frac{\kappa-1}{\kappa}} \tag{38}$$

which results from the Fourier transform of eq.(36).

This concludes our statistical mechanical account for the critical fluctuations in terms of cluster formation, for each of the two alternative evolution schemes. We shall proceed, in the next section, to discuss corresponding numerical studies, pertaining to a critical component for pion production in A+A collisions through simulations of a Monte-Carlo type. Our expectation is that the 'theoretical generation' of events whose origin lies exclusively in a critical state reached by the QGP system, will aid the search for respective signals in produced multiparticle pion states.

6. Monte-Carlo simulations

Following the considerations in the previous sections it becomes obvious that the formation of critical clusters is expected to induce direct phenomenological consequences, in the multiplicity distribution of the produced sigmas, in the final states of a $A + A$ collision. In the first part of the present section we shall describe the development of a Monte-Carlo programme for the purpose of simulating the production of "critical pions" in such collision processes, coming from the decay of light sigmas. The reader who is not interested for the technical details of our approach can skip the first subsection and go directly to the next one where we discuss a proposed algorithm for detecting the critical fluctuations in experimental data.

6.1. CMC Generator for critical events

In the context of the QCD phase diagram in the temperature/chemical potential plane, a two step procedure is required for the study of the critical pion spectrum formation. First, we need to produce the clusters corresponding to the σ-condensates. According to our theoretical discussion, the geometry of the σ-clusters is determined by the evolution pattern of the centrally formed fluid of quarks and gluons. In the case of longitudinal evolution we have a cylindrical arrangement of several clusters in the transverse momentum $\otimes$ rapidity space (cf. sections 3 and 4) while in a spherically symmetric evolution a single cluster in momentum space is formed (cf. section 5).

Second, we let the sigmas in the condensates decay into pions with a branching ratio 1:2 for neutral to charged pion production. The crucial parameter for determining the spectrum of the produced pions is provided by the mass of the decaying sigmas. As the sigma mass is not a constant but, *in fact*, evolves during the freeze-out process, we treat it as a varying parameter in our numerical considerations.

We recall that the number of clusters in the case of cylindrical symmetry is determined by the size of the critical region while the multiplicity of σ's within each cluster depends on the couplings occuring in the free energy of the system at the critical point. Once the sigma mass is assigned a specific value, we use two-body phase space kinematics in order to determine the transverse momenta and the rapidities of the pions. For the spherically symmetric case, on the other hand, a single critical cluster is formed around the CM

of the system ($\vec{p} = 0$) while the multiplicity within the cluster depends, once again, on the couplings of the "critical" free energy. In what follows we shall conduct numerical investigations, using Monte-Carlo methodology, for both the cylindrical and the spherical configurations of the critical clusters. It could very well be that the geometry of the evolving critical system is neither perfectly cylindrical nor spherical but consistent with a picture interpolating between these two extreme regimes.

Let us consider the implementation of the first step (simulation of the sigma-condensates) for a longitudinally expanding critical system (cylindrical geometry). The input parameters determining the sigma-distribution are: the size $R_\perp$ of the system in the transverse direction, the total rapidity interval Δ, the proper time scale τ, the critical temperature T_c, the coupling g in the 3-D Ising effective free energy and the isothermal critical exponent δ. Once we fix the values of the input parameters we can calculate the size of a cylindrical cluster of sigmas, meaning its transverse momentum radius $|\Delta\vec{p}_\perp|$, given by eq.(32), and its size in rapidity $2\Delta_u$ (see eq.(16)). The number of sigma clusters in the transverse (momentum or real) space projection of the critical system, as well as the corresponding number of clusters in rapidity space are then given through eqs.(23). Finally, the multiplicity of sigmas within each cluster can be obtained using eq.(22).

Next, we construct the phase space projections of the sigmas in the critical event. The determination of the rapidity space profile proceeds as follows: We produce a configuration of $N_\parallel$ centers for these clusters treating them as random variables, uniformly distributed in $[0, \Delta]$ according to eq.(26). Then we generate around each center the sigmas, distributed with a density-density correlation following the power-law (15).

This stage of the algorithm requires the construction of a random fractal with a given fractal dimension d_F. In order to perform this construction we have to use test-functions of the form $P(x) \sim x^{-1-d_F}$ as a generalization of the Lévy distributions for arbitrary embedding dimension [19]. We produce randomly the rapidities corresponding to one cluster using the appropriate test-function. In general, the resulting set does not have the correct center and size. Due to self-similarity the cluster size is obtained through a simple scaling while, with a suitable translation, the cluster is placed around the corresponding center. Coalescence of neighbouring clusters *is* allowed, so the actual multiplicity within each cluster depends on the position of the centers of its neighbours. Therefore, the cluster arrangement in the rapidity space determines the total multiplicity N_σ of sigmas in the event.

Turning our attention to the transverse momentum space we arrange the centers of the $N_\perp$ clusters so that they are distributed according to the exponential law (30), under the constraint that the total transverse momentum of the centers vanishes. To each such cluster correspond $\frac{N_\sigma}{N_\perp}$ sigma-particles distributed according to the power-law (20). The construction algorithm for the transverse momentum clusters is analogous to the algorithm used for the construction in rapidity space. The test-function has to be adjusted to produce the random fractal with the correct dimension.

We, therefore, end up with two sets of phase space variables. A set S_T with N_σ transverse momentum variables $\{(p_{T,x_1}, p_{T,y_1}),\ (p_{T,x_2}, p_{T,y_2}), ...,\ (p_{T,x_{N_\sigma}}, p_{T,y_{N_\sigma}})\}$ and a set S_ξ with N_σ rapidity variables $\{\xi_1,\ \xi_2, ...,\ \xi_{N_\sigma}\}$. The sigma-content of a "critical" event, respecting the cartesian product form of the underlying cylindrical geometry, is then realized as any possible one-to-one pairing of the elements of S_T with the elements of S_ξ.

For a spherically symmetric expansion the size of the critical cluster is represented by a single parameter R corresponding to the radius of the (growing) system in the 3-D space. This makes the case in hand much easier to handle. First we specify the size $|\Delta\vec{p}|$ of the (single) critical sigma cluster in momentum space, cf. eq.(37) and then using eq.(35) we determine the total sigma multiplicity N_σ within this cluster. The generation of the momenta of the sigma-particles is then based on the observation that for the 3-D system the density-density correlation function in momentum space coincides with the step distribution of a Lévy flight [19] leading to a fractal set with the same fractal dimension ($\tilde{d}_F^{(3)} \approx 1$). Thus the algorithm used for the generation of the σ-momenta is given through the following equations

$$\begin{aligned} p_{x,i} &= p_{x,i-1} + |\Delta\vec{p}| r_1 \sqrt{1-r_2^2}\cos(2\pi r_3) \\ p_{y,i} &= p_{y,i-1} + |\Delta\vec{p}| r_1 \sqrt{1-r_2^2}\sin(2\pi r_3) \\ p_{z,i} &= p_{z,i-1} + |\Delta\vec{p}| r_1 r_2 \end{aligned} \tag{39}$$

where r_1 is distributed according to the density-density correlation function (38), r_3 is random variable uniformly distributed in $[0,1]$ while r_2 is uniformly distributed in $[-1,1]$. A final scaling and translation, as in the case of the cylindrical clusters, is needed in order to embed the cluster in a region with radius $|\Delta\vec{p}|$ around $\vec{p}=0$ in momentum space.

In order to establish contact with the observables in an experiment with colliding relativistic heavy ions we must take into account the decay of sigmas into pions. As already discussed this constitutes a straight forward step for a given value of the mass of the decaying sigmas. If this mass is far from the pion production threshold $2m_\pi$ the kinematics of the pions is strongly influenced by the sigma-mass and the fluctuation pattern of the pions is disordered relative to the spectrum of the sigmas. On the other hand, the sigma mass is generated dynamically during the freeze-out phase and, if the decay rate is much larger than the expansion rate, there is a good possibility that the sigmas decay immediately after their effective mass has reached the pion production threshold [15]. If this is the case then the fluctuation patterns describing the sigma momenta are transfered, almost unchanged, to the momenta of the produced pions. Here however, we will follow a more general mechanism for the decay of the sigmas allowing us also to describe a more conservative scenario when the sigmas decay well above the two pion threshold. Specifically, in order to simulate the variation of the sigma mass during the freeze-out process, we introduce a probability distribution $P(M_\sigma)$ determining the number of sigmas with mass M_σ which decay into pions. We assume that $P(M_\sigma)$ is well described by a Gaussian of mean value M_σ and variance δm_σ.

The generation of the critical events is therefore completed in the last stage of our Monte-Carlo code (CMC) when, treating the sigma mass as a random variable with propability density $P(M_\sigma)$, we produce the final charged pions through the decay of the critical sigmas. The quantum mechanical amplitude describing the probability of the sigma-decay into a π^+-π^- pair is supposed to be independent of the sigma-momentum.

6.2. Reconstruction of the critical σ-sector

Using the CMC algorithm we produce a large number of critical events and we study their phenomenology. Our main interest is to reveal the critical fluctuations from the

momenta of the final observed charged pions. For this purpose we perform an event-by-event intermittency analysis in the factorial moments of the negative pion momenta looking for a region with self-similar fluctuations. If the mass parameter M_σ is less than $1\ MeV$ above the two pion threshold the critical fluctuations can be directly observed in the momenta of the negative pions. Increasing M_σ the effect gets more and more suppressed leading, relatively soon ($M_\sigma \approx 10\ MeV\ +\ 2m_\pi$), to an almost dissapearance of the critical fluctuations (see Fig. 5, open up triangles). This behaviour remains even if the variance δm_σ vanishes. If we increase δm_σ for a given value of M_σ we find, in general, a suppression of the critical region with rate depending on the value of M_σ. If $M_\sigma \leq 1\ MeV + 2m_\pi$ the rate of suppression is very small and the critical fluctuations, for realistic values of δm_σ, practically persist. In order to get back the critical behaviour one has, therefore, to reconstruct the critical sigmas based on the momenta of the observed charged pions. We propose the following reconstruction algorithm:

- For a given event, using as input the momenta of the charged pions, form the invariant mass $m^2_{\pi^+\pi^-} = (p_+ + p_-)^2$ for all possible pairs of π^+-π^- (p_+ (p_-) is the 4-momentum of π^+ (π^-)).

- Determine the probability distribution of the quantity $m^2_{\pi^+\pi^-}$. Look for a peak in the distribution. Form a new set of charged pions picking up the π^+-π^- pairs within a region of a few MeV ($\approx 50\%\delta m_\sigma$) around the peak. Not all of these pairs correspond to critical sigmas, but, according to the decay scenario described above, most of the critical sigmas certainly belong to this set.

- Adding up the momenta of the selected charged pions form the momenta of the corresponding (fictitious) sigmas $p_\sigma = p_+ + p_-$.

- Perform a factorial moment analysis to the momenta of the fictitious sigmas. Due to the presence of the critical sigmas in this set, a strong intermittency effect shows up in the sigma sector (see Fig. 5, full circles) with the expected indices.

7. Numerical results

Having developed both a Monte-Carlo generator for critical events and an algorithm for the restoration of the critical sigma sector in an event-by-event analysis we shall now proceed to present our numerical results, showing the phenomenological impact of our theoretical investigations. Let us first specify values for our input parameters, which correspond to the critical exponent δ, the effective coupling g, the transverse radius $R_\perp$, the proper time scale τ, the size in rapidity Δ and the critical temperature T_c. The first two parameters are fixed, on the basis of universality class arguments, to the values of the 3-D Ising model: $\delta \approx 5$ and $g \approx 2$ [12,13]. The critical temperature is taken $T_c \approx 140\ MeV$. The size in rapidity is determined so as to meet the conditions at the RHIC collider: $\Delta \approx 11$. Finally we choose: $R_\perp \approx 22\ fm$ and $\tau \approx 17\ fm$. It follows that the presented results are predictions for the event-characteristics in RHIC, provided that the critical point is there accessible. The above choice of $R_\perp$ and g leads us to the value $R_u \approx 13\ fm$. This value implies the formation of 2 clusters in the transverse momentum projection. Taking into account that $\Delta_u \approx 0.55$ we find 10 clusters in the rapidity projection. Thus

approximately 20 critical clusters are expected to be formed in RHIC conditions, adopting the cylindrical evolution scenario. Our numerical results are exhibited in a series of figures and pertain to a large set of critical events produced through the CMC algorithm and using parameter values appropriate for RHIC. We investigate separately the two possible geometries, cylindrical and spherical, for the evolution of the critical fluid.

Case of cylindrical symmetry: We produce 10000 "critical" events and perform an event-by-event factorial moment analysis for the sigma clusters. Our results are depicted in Figs. 1-3. The mean multiplicity of sigmas turns out to be ≈ 90. In Fig. 1a we present the inclusive rapidity spectrum of the sigmas for the set of the 10000 events. The uniform central plateau indicates the cancelling of the fluctuations in the inclusive distribution. In Fig. 1b we show the inclusive distribution of the sigmas in p_T.

In Figs. 2a,b results of the event-by-event factorial moment analysis in rapidity space and in transverse momentum space for the whole set of the 10000 "critical" events are displayed. In Fig. 2a we present the distribution of the slopes in a linear fit for $\ln(F_2^{(1)}(M))$ as a function of $\ln(M)$ (M beeing the number of bins in rapidity) for all events. We observe a clear maximum near $s_2^{(1)} \approx 0.27$ and a mean variance $\delta s_2^{(1)} \approx 0.05$. This picture is consistent with the formation, in most events, of a complex structure with fractal dimension $d_F^{(1)} \approx 0.73$ which is close to the mass dimension $d_F^{(1)} = \frac{2}{3}$ obtained for a single sigma cluster (see eq.(15)) in rapidity. In Fig. 2b the analogous analysis is made for the distribution of the sigmas in transverse momentum space. The corresponding histogram gives the distribution of $s_2^{(2)}$ for the slopes determined after a linear fit to the logarithm of the two dimensional moment $F_2^{(2)}(M)$ as a function of the logarithm of M. We see, once more, a peaked distribution with a maximum at about $s_2^{(2)} \approx 1.23$. This distribution is slightly broader than the corresponding distribution in rapidity. The mean value (1.23) indicates a fractal structure with dimension $d_F^{(2)} \approx 0.77$ close to the mass dimension of a single cluster in p_T ($d_F^{(2)} = \frac{2}{3}$). For completeness we mention that for the azimuth angle in transverse momentum space we get a totally uniform inclusive distribution, as one would expect.

Putting pions into the picture we give, in Figs. 3a,b, the results of the event-by-event factorial moment analysis (a) in rapidity and (b) in p_T of the negative pion momentum distribution. To determine the decay of sigmas into pions according to the distribution $P(M_\sigma)$ we use the parameter values $M_\sigma \approx 285\ MeV$ and $\delta m_\sigma \approx 5\ MeV$. As pion mass we have used $m_\pi = 140\ MeV$. For the mean value of $s_2^{(1)}$ in the rapidity space analysis of π^- we find $< s_2^{(1)} > \approx 0.07$ (see Fig. 3a) while for the case of the transverse momentum we find $< s_2^{(2)} > \approx 0.17$ (see Fig. 3b). These values should be compared with the values $< s_2^{(1)} > \approx 0.27$ and $< s_2^{(2)} > \approx 1.23$ respectively, found in the event-by-event analysis of the sigmas. We see a clear tendency for suppression of the dynamical fluctuations in favour of the statistical ones in the pionic sector.

To recover the dynamical fluctuations one has to apply the sigma-recontruction algorithm described in the previous paragraph. To investigate the suppression and the restoration of the critical fluctuations we compute the dependence of $< s_2^{(2)} >$ for the reconstructed sigmas on the quantity δm_σ, keeping a fixed value $M_\sigma = 290\ MeV$. The analysis is performed for classes (constant δm_σ) with 500 events each. Our results are presented in Fig. 4 (full squares). In the same plot we show the best fit using the Boltzmann

function $f(x) = \frac{A_1 - A_2}{1+e^{(x-x_o)/d}} + A_2$ (dashed line). The fit parameters converge to the values: $A_1 = 2.12$, $A_2 = 0.35$, $x_o = 0.08$ and $d = 1.1$. The nonvanishing value of A_2 shows that, even if δm_σ becomes very large, a clear intermittency signature ($< s_2^{(2)} > \geq 0.35$) is present in the reconstructed events. Of course the asymptotic value of $< s_2^{(2)} >$ depends on M_σ and decreases rapidly as M_σ is increased.

To illustrate this effect more transparently we present in Fig. 5 the second factorial moment in transverse momentum space for a typical critical event taking $M_\sigma = 290\ MeV$, $\delta m_\sigma = 5\ MeV$ and $m_\pi = 140\ MeV$. We see that although the fluctuations in π^- (open up triangles) are strongly suppressed they are practically revealed in the sector of the reconstructed sigmas (full circles).

Spherically symmetric evolution: In Figs. 6a,b we give the rapidity (a) and transverse momentum (b) inclusive distributions for the sigmas in a set of 10000 Monte-Carlo generated events. The distribution in rapidity is very interesting. The formation of a single source (cluster) of sigmas in the collision process leads to an almost Gaussian shape which is very clearly distinguished from the plateau emerging in the case of many sources (cylindrical symmetry). Such differences in the rapidity distribution are also observed between $p-p$ and heavy-ion collision experiments far from the critical point. Our explanation is that the multiparticle production in $p-p$ is dominated by the formation of a single source while in heavy-ion collisions there are many sources involved (supporting the scenario of longitudinal expansion).

Finally, in Figs. 7a,b we present the factorial moment analysis in the sigma sector for the set of the 10000 MC events presented in Figs. 6a,b. We find $< s_2^{(1)} >= 0.14$ for the rapidity distribution and $< s_2^{(2)} >= 0.99$ for the transverse momentum distribution. A suppression of the fluctuations in the rapidity space is clearly observed. This is a peciularity of the spherical geometry as discussed in the previous section.

In summary we have shown that even if the sigmas, which are expected to be formed in a heavy ion collision experiment, as the critical point is approached, decay well above the two-pion threshold, it is possible, by investigating the momentum distribution of the produced charged pions, to (partially) reconstruct the critical sigma sector and to restore the corresponding critical fluctuations.

8. Concluding remarks

In this work we have explored the idea that pion production in heavy ion collisions may have a component whose source can be asrcibed to a critical QCD phase. Our working hypothesis has been that density fluctuations near the QCD critical point should leave their imprints on the observed pion spectrum. Encouraged from the accumulating evidence, through microscopically-based theoretical investigations, lending support to a phase diagram in which critical QCD behaviour does occur we focused our efforts on establishing a linkage between critical fluctuations and intermittency patterns in pion production. Such a proposal pertains, of course, to one of two components characterizing the pion spectrum in $A + A$ collisions, as conventional production mechanisms are also expected to take place.

The methodology employed in this work centered itself on the statistical mechanical aspects of the problem. We have chosen to rely on the strategy of critical cluster formation

which seems to be the most advantageous one given the finite size aspects of the system under study. In the context of the currently accepted theoretical proposal that the universality class of the critical QCD system is represented by the 3-D Ising model, we have both established connections with pion production ascribed to the aforementioned unconvential component and explored its observability in terms of specific filters associated with a reasonably wide window for the σ-mass. Employing Monte-Carlo type numerical methodologies we have arrived at specific *testable* predictions which can be checked against forthcoming data in heavy ion experiments. In practical terms our present undertaking can be viewed as having a dual prospective. On the one hand, it aims at isolating a specific type of signal in the constitution of the final states with an unconventional origin which would give evidence in favor of an antecedent QGP phase. On the other, it could serve as a guide towards the identification of the source (critical point?) responsible for long range correlations in the QCD phase diagram [11].

The fact that the pions constitute the focal point of our approach is also significant from a purely phenomenological point of view addressing itself directly to the study of the constitution of the multiparticle spectrum (particle multiplicities and particle ratios) produced in very high energy collisions, especially $A+A$. In this connection, thermodynamical analyses from the hadronic perspective which base themselves on thermal equilibration assumptions for the produced multiparticle system are of special interest. Pioneering studies in this direction [20] have assumed an ideal hadron gas model and have produced satisfactory results, lending credit to the thermal equilibration premise, but are in no position to evaluate whether or not the source of the resulting multiparticle system is located inside or outside (QGP?) the hadronic domain.

Recently, the same type of analysis has been conducted [21] within the framework of Hagedorn's Statistical Bootstrap Model (SBM) [22] once the latter was extended so as to include the strangeness quantum number. This approach not only incorporates, via a self-consistent logic, interactions into the resulting thermodynamical system but also sets limit for the hadronic phase of matter. According to the results of [21] there is an accumulation, in the plane of thermodynamical variables specified by temperature and light quark chemical potential, of points from S+S, S+Ag and (preliminary) Pb+Pb experimental data from SPS at CERN on either side of the curve that separates the hadronic world from a different phase of matter. Matching such results from the QCD side certainly specifies a task worthwhile pursuing (suggesting a first order transition).

Looking ahead, we assess as the most pressing question in relation to our proposed scheme to be the following. If, according to the present theoretical evidence, the second order phase transition achieved by the QGP system in the temperature-baryon chemical potential plane is a critical point marking the end of a first order transition curve, are there realistic prospects of observing the component contributing to pion production presently investigated? Clearly, the answer depends as to whether one can define a reasonably 'wide' window around such a critical point within which visible implications can be formulated. This constitutes a problem of interest which is currently being investigated. At the same time, we believe that the methodology developed in this paper has a wider impact as it can be easily adopted to any future scenario concerning the, still open, issue of QCD universality classes implicated as being realized in $A + A$ collisions.

REFERENCES

1. A. Bialas and R. Peschanski, Nucl. Phys. B273 (1986) 703; Nucl. Phys. B308 (1988) 857.
2. J.D. Bjorken, Phys. Rev. D27 (1983) 140.
3. L.D. Landau and E.M. Lifshitz, *Statistical Physics*, Pergamon Press, Oxford, Third Edition, 1980.
4. T. Schäfer, Phys. Rev. D57 (1998) 3950; M. Alford, K. Rajagopal and F. Wilczek, Phys. Lett. B422 (1998) 247; hep-ph/9804403; T. Schäfer and F. Wilczek, hep-ph/9810509.
5. F. Wilczek, Int. J. Mod. Phys. A7 (1992) 3911; F. Wilczek, Nucl. Phys. A566 (1994) 123c.
6. J. Berges, D.-U. Jungnickel and C. Wetterich, Phys. Rev. D59 (1999) 034010; Eur. Phys. J. C13 (2000) 323.
7. J. Berges and K. Rajagopal, Nucl. Phys. B538 (1999) 215.
8. M.A. Halasz, A.D. Jackson, R.E. Shrock, M.A. Stephanov and J.J.M. Verbaarschot, Phys. Rev. D58 (1998) 096007.
9. N.G. Antoniou, C.N. Ktorides, I.S. Mistakidis and F.K. Diakonos, Eur. Phys. J. C4 (1998) 513; N.G. Antoniou, F.K. Diakonos, C.N. Ktorides and M. Lahanas, Phys. Lett. B432 (1998) 8.
10. K. Rajagopal and F. Wilczek, Nucl. Phys. B399 (1993) 395; Nucl. Phys. B404 (1993) 577.
11. M.A. Stephanov, K. Rajagopal and E. Shuryak, Phys. Rev. Lett. 81 (1998) 4816; F. Wilczek, Nature 395 (1998) 220-221.
12. M.M. Tsypin, Phys. Rev. Lett. 73 (1994) 2015.
13. J. Berges, N. Tetradis and C. Wetterich, Phys. Rev. Lett. 77 (1996) 873.
14. D.J. Scalapino and R.L. Sugar, Phys. Rev. D8 (1973) 2284; J.C. Botke, D.J. Scalapino and R.L. Sugar, Phys. Rev. D9 (1974) 813.
15. N.G. Antoniou, Y.F. Contoyiannis and F.K. Diakonos, Nucl. Phys. A661 (1999) 399c.
16. N.G. Antoniou, Nucl. Phys. B77 (1999) 307c.
17. N.G. Antoniou, Y.F. Contoyiannis, F.K. Diakonos and C.G. Papadopoulos, Phys. Rev. Lett. 81 (1998) 4289; N.G. Antoniou, Y.F. Contoyiannis and F.K. Diakonos, Phys. Rev. 62E (2000) 3125.
18. T. Vicsek, *Fractal growth phenomena*, World Scientific, 1989; K. Falconer, *Fractal geometry*, John Wiley and Sons, 1989.
19. M.F. Shlesinger, G.M. Zaslavsky and U. Frisch, *Lévy Flights and Related Topics in Physics*, Springer-Verlag, Heidelberg 1995.
20. R. Fiore, R. Page and L. Sentorio, Nuovo Cimento A 37A (1977) 399; J. Letessier, A. Tounsi and J. Rafelski, Phys. Lett. B292 (1992) 417; J. Cleymans and H. Satz, Z. Phys. C57 (1993) 135; J. Sollfrank, M. Gaździcki, U. Heinz and J. Rafelski, Z. Phys. C61 (1994) 659; F. Becattini, Z. Phys. C41 (1996) 485.
21. A.S. Kapoyannis, C.N. Ktorides and A.D. Panagiotou, Phys. Rev. C58 (1998) 2879; Phys. Rev. D58 (1998) 034009.
22. R. Hagedorn, Suppl. Nuovo Cimento 3 (1965) 147; R. Hagedorn and J. Ranft, Suppl. Nuovo Cimento 6 (1968) 311; R. Hagedorn and J. Ranft, Nucl. Phys. B48 (1972) 157.

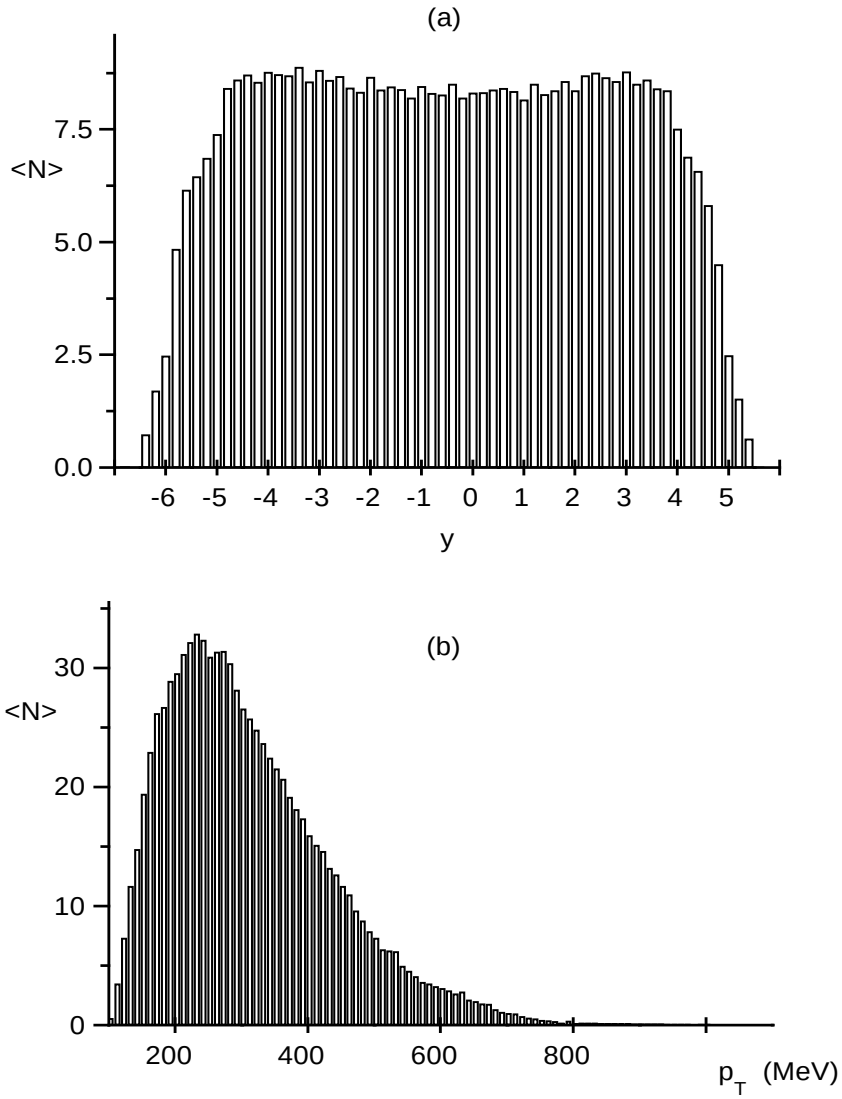

Figure 1. (a) The rapidity distribution of the σ-particles in 10000 Monte-Carlo (MC) generated critical events (cylindrical geometry is assumed to be valid). (b) The corresponding inclusive transverse momentum distribution.

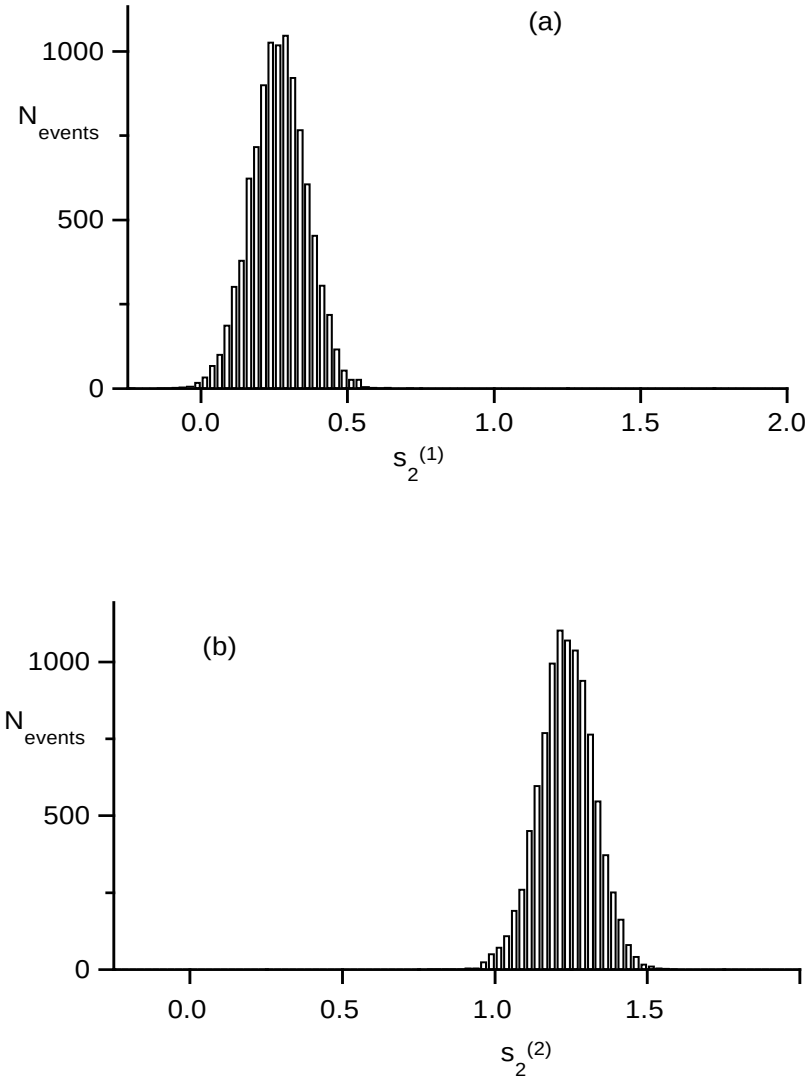

Figure 2. (a) The distribution of the slope $s_2^{(1)}$ resulting from a linear fit of $\ln(F_2^{(1)})$ vs. $\ln(M)$ in an event-by-event factorial moment analysis of the σ-particles in rapidity for the 10000 MC events (M is the number of bins). (b) The distribution of the slope $s_2^{(2)}$ obtained in the analogous analysis in transverse momentum space for the same set of events as in Fig. 2a.

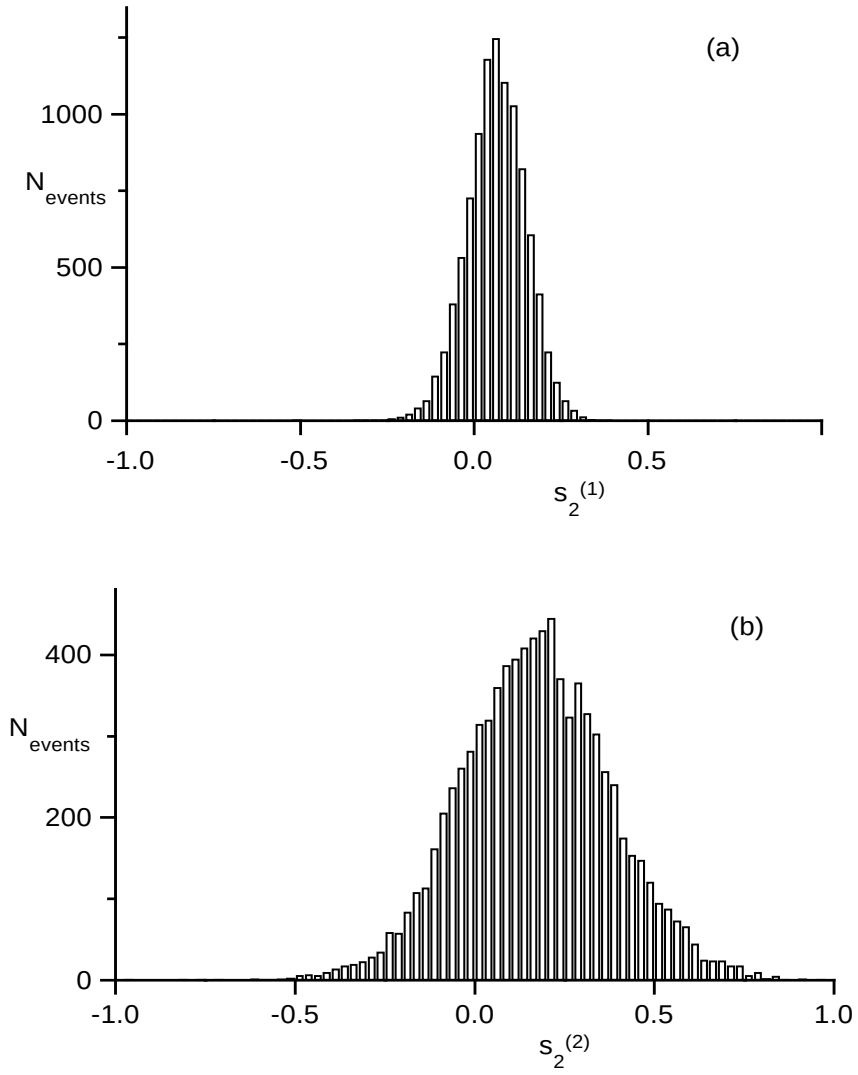

Figure 3. (a) The distribution of the slope $s_2^{(1)}$ resulting from a linear fit of $\ln(F_2^{(1)})$ vs. $\ln(M)$ in an event-by-event factorial moment analysis of the negative pions in rapidity for the 10000 MC events (the same as in Figs. 1,2). (b) The distribution of the slope $s_2^{(2)}$ resulting from a linear fit of $\ln(F_2^{(2)})$ vs. $\ln(M)$ in a 2-D event-by-event factorial moment analysis of the negative pions in transverse momentum space.

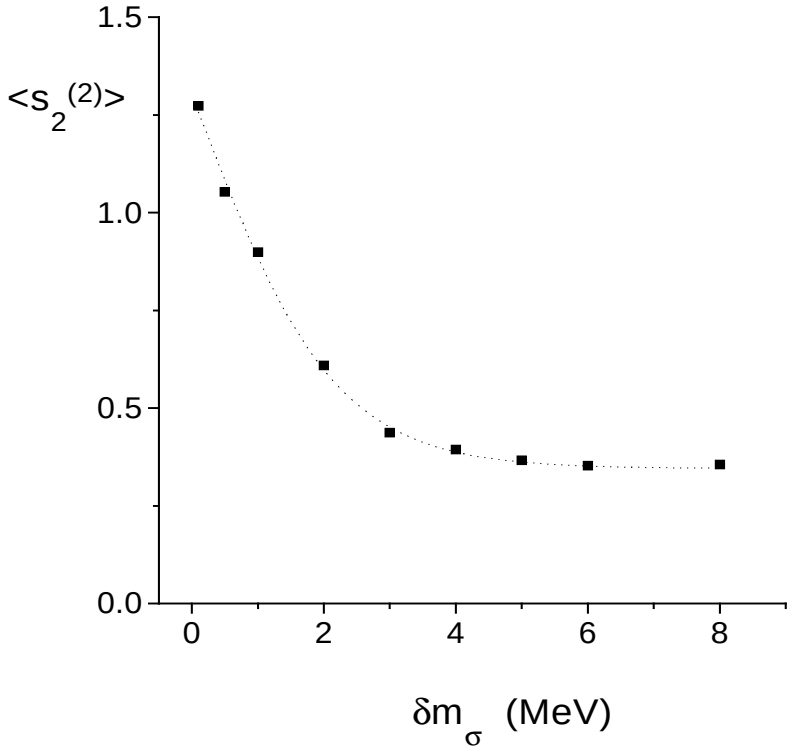

Figure 4. The dependence of $< s_2^{(2)} >$ on δm_σ (full squares) calculated with sets each consisting of 500 critical events generated with the cylindrically symmetric algorithm. M_σ is taken 290 MeV. A fit with the Boltzmann function (dashed line) is also shown.

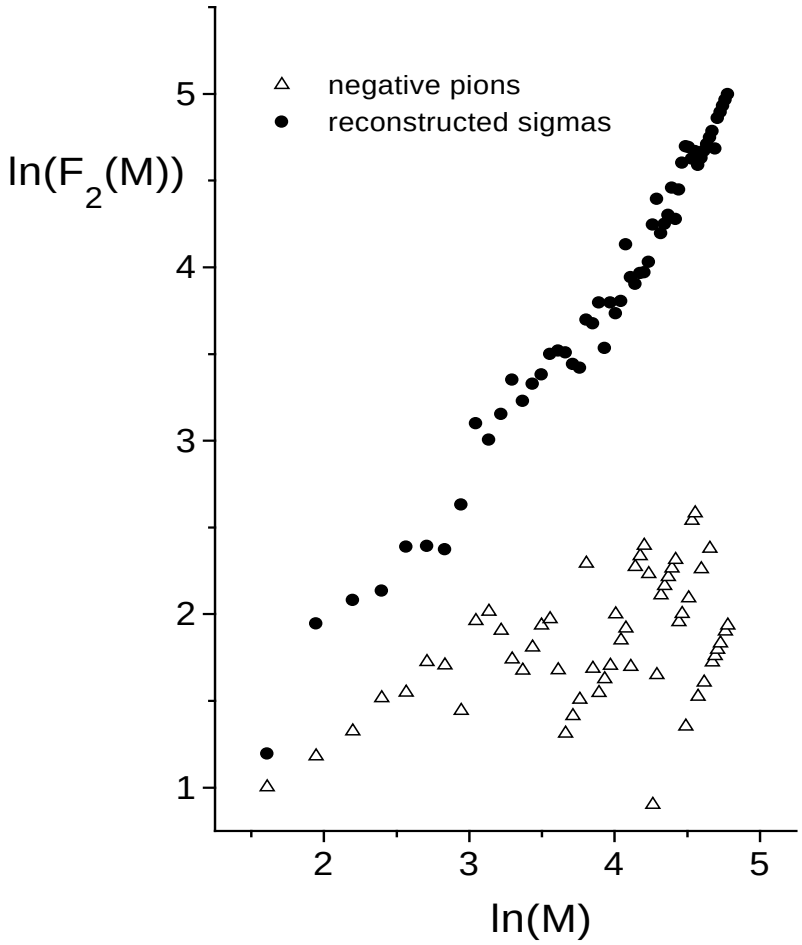

Figure 5. The second factorial moment in transverse momentum space for a critical event (negative pions) obtained through the cylindrically symmetric CMC generator and corresponding to $M_\sigma = 290\ MeV$, $\delta m_\sigma = 5\ MeV$ (open up triangles). The corresponding moment in the sigma-sector obtained through the above described reconstruction algorithm is also shown (full circles). The restoration of the critical fluctuations is clearly displayed.

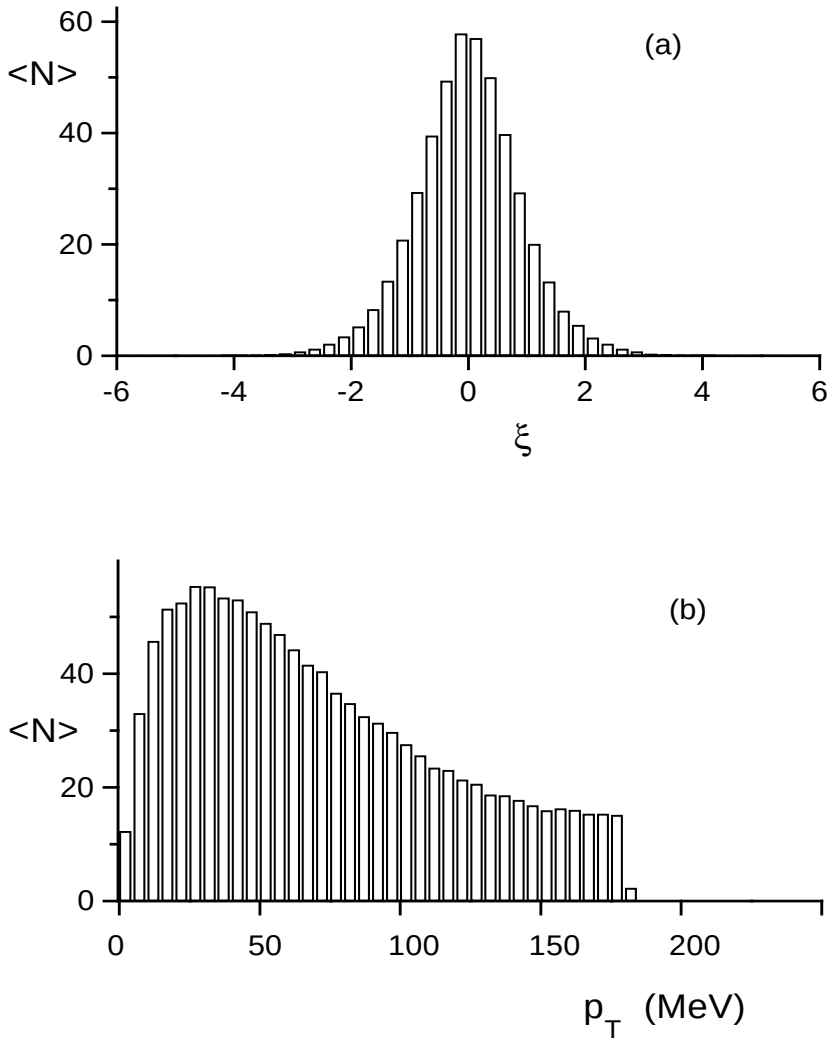

Figure 6. Inclusive distributions in (a) rapidity and (b) magnitude of the transverse momentum of the σ-particles for 10000 Monte-Carlo generated critical events assuming spherical symmetry.

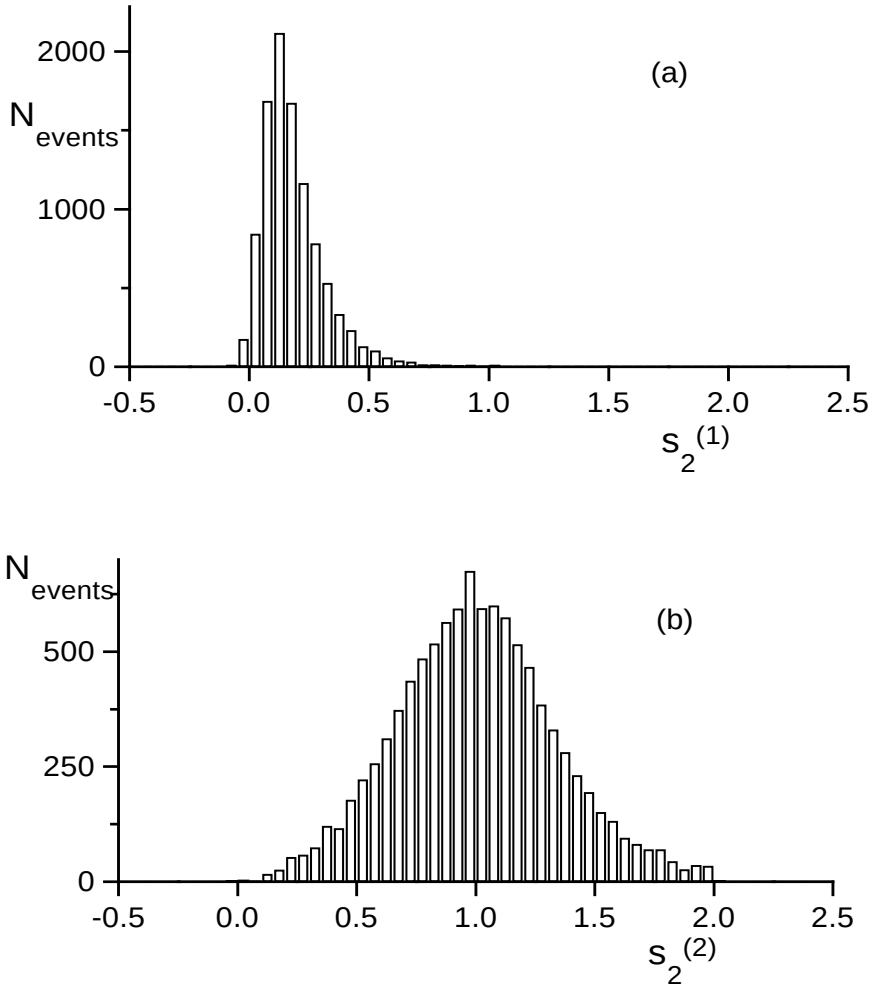

Figure 7. (a) The distribution of the slope $s_2^{(1)}$ resulting from a linear fit of $\ln(F_2^{(1)})$ vs. $\ln(M)$ in an event-by-event factorial moment analysis of the sigmas in rapidity for 10000 MC events with spherical evolution. (b) The distribution of the slope $s_2^{(2)}$ resulting from a linear fit of $\ln(F_2^{(2)})$ vs. $\ln(M)$ in a 2-D event-by-event factorial moment analysis of the sigmas in transverse momentum space for the same set of events as in (a).